Article

Bone marrow CD169+ macrophages promote the retention of hematopoietic stem and progenitor cells in the mesenchymal stem cell niche

Andrew Chow,[1,2,3] Daniel Lucas,[2,3] Andrés Hidalgo,[2,4]
Simón Méndez-Ferrer,[2,5] Daigo Hashimoto,[1,2] Christoph Scheiermann,[2,3]
Michela Battista,[2] Marylene Leboeuf,[1,2] Colette Prophete,[2,3]
Nico van Rooijen,[6] Masato Tanaka,[7] Miriam Merad,[1,2]
and Paul S. Frenette[2,3]

[1]Department of Gene and Cell Medicine and [2]Department of Medicine, Mount Sinai School of Medicine, New York, NY 10029
[3]Ruth L. and David S. Gottesman Institute for Stem Cell and Regenerative Medicine Research, Albert Einstein College
 of Medicine, Bronx, NY 10461
[4]Department of Epidemiology, Atherothrombosis, and Imaging and [5]Cardiovascular Developmental Biology Department,
 Centro Nacional de Investigaciones Cardiovasculares, 28029 Madrid, Spain
[6]Department of Molecular Cell Biology, Vrije Universiteit, 1081 HV Amsterdam, Netherlands
[7]Laboratory for Innate Cellular Immunity, RIKEN Research Center for Allergy and Immunology, Yokohama, Kanagawa,
 230-0045, Japan

Hematopoietic stem cells (HSCs) reside in specialized bone marrow (BM) niches regulated by the sympathetic nervous system (SNS). Here, we have examined whether mononuclear phagocytes modulate the HSC niche. We defined three populations of BM mononuclear phagocytes that include Gr-1^{hi} monocytes (MOs), Gr-1^{lo} MOs, and macrophages (MΦ) based on differential expression of Gr-1, CD115, F4/80, and CD169. Using MO and MΦ conditional depletion models, we found that reductions in BM mononuclear phagocytes led to reduced BM CXCL12 levels, the selective down-regulation of HSC retention genes in Nestin+ niche cells, and egress of HSCs/progenitors to the bloodstream. Furthermore, specific depletion of CD169+ MΦ, which spares BM MOs, was sufficient to induce HSC/progenitor egress. MΦ depletion also enhanced mobilization induced by a CXCR4 antagonist or granulocyte colony–stimulating factor. These results highlight two antagonistic, tightly balanced pathways that regulate maintenance of HSCs/progenitors in the niche during homeostasis, in which MΦ cross talk with the Nestin+ niche cell promotes retention, and in contrast, SNS signals enhance egress. Thus, strategies that target BM MΦ hold the potential to augment stem cell yields in patients that mobilize HSCs/progenitors poorly.

CORRESPONDENCE
Paul S. Frenette:
paul.frenette@einstein.yu.edu
OR
Miriam Merad:
miriam.merad@mssm.edu

Abbreviations used: BMDM, BM-derived MΦ; BMEF, BM extracellular fluid; DT, diphtheria toxin; G-CSF, granulocyte colony-stimulating factor; HSC, hematopoietic stem cell; MΦ, macrophage; MO, monocyte; Q-PCR, quantitative RT-PCR; SNS, sympathetic nervous system.

The BM is the preferred site for adult hemato-poiesis. Transplantation of BM cells containing hematopoietic stem cells (HSCs) and progenitors has been a remarkable medical advancement that allows for the replacement of the hematopoietic compartment after preparative regimens. HSCs are retained in perivascular niches that are distributed near osteoblasts and within the nonendosteal parenchyma (Kiel et al., 2005; Sugiyama et al., 2006; Lo Celso et al., 2009; Méndez-Ferrer et al., 2010b). The ability

to mobilize HSCs/progenitors out of the BM into the peripheral blood has allowed for efficient, less invasive HSC procurement in clinical stem cell transplantation. However, up to 30% of patients previously treated with cytotoxic anticancer therapies do not mobilize sufficient numbers of stem cells using current protocols (Bensinger et al., 2009).

A. Chow and D. Lucas and M. Merad and P. Frenette contributed equally to this paper.

JEM

Sympathetic neural tone is crucial for both steady state (Méndez-Ferrer et al., 2008) and granulocyte colony-stimulating factor (G-CSF)–enforced (Katayama et al., 2006) release of HSCs/progenitors from the BM. Recent studies indicate that mesenchymal stem cells (MSCs), identified by the expression of the intermediate filament protein Nestin, comprise a critical cellular constituent of the stem cell niche that is under the control of the sympathetic nervous system (SNS; Méndez-Ferrer et al., 2010b). Because previous studies using G-CSF receptor–deficient mice showed that expression of the receptor on transplantable hematopoietic cells was required for G-CSF–induced mobilization (Liu et al., 2000), we have previously speculated that at least two distinct pathways, neural and hematopoietic, acted in concert to promote HSC/progenitor egress (Katayama et al., 2006).

Hypothesizing that mononuclear phagocytes are crucial for stromal function of the BM, we sought to eliminate these populations to evaluate their contributions to HSC trafficking. Unexpectedly, we have found that BM macrophages (MΦ) did not promote the egress of HSCs/progenitors, but rather contributed to the retention of HSCs in the BM by acting on Nestin[+] MSCs. These data uncover a new role for the innate immune system in regulating stem cell niche functions.

RESULTS

Phenotypic markers of BM mononuclear phagocytes

Depletion of monocytes (MO) and/or MΦ from the BM has been accomplished with injection of clodronate liposomes (Giuliani et al., 2001) and injection of the FK-binding protein dimerizer AP20187 in transgenic Mafia mice (Burnett et al., 2004; Chang et al., 2008). Mafia mice have a Fas suicide/apoptotic system driven by the CD115 (M-CSF receptor) promoter. Previous phenotypic descriptions of BM MΦ have exclusively relied on F4/80 expression (Hume et al., 1983; Giuliani et al., 2001; Chang et al., 2008). However, this marker is also expressed on BM neutrophils (Gr-1^{+}CD115^{−}), Gr-1^{hi} MO (Gr-1^{+}CD115^{+}), Gr-1^{lo} MO (Gr-1^{−}CD115^{+}; Gordon and Taylor, 2005), and eosinophils (SSC^{hi}Siglec-F^{+}; Zhang et al., 2004; Fig. S1). To distinguish among BM mononuclear phagocytes and to elucidate their differential surface phenotypes, we purified different BM populations via cell sorting based on three markers: Gr-1 (Ly6C/G), CD115, and F4/80. As expected, neutrophil granulocytes were homogenously represented in the Gr-1^{+}CD115^{−} gate (Fig. 1 A, gate I) and represented 49.6 ± 1.1% of the total BM nucleated cells. In mice, there are two subsets of CD115^{+} MO that differentially express Gr-1 (Gordon and Taylor, 2005). In concordance, the Gr-1^{+}CD115^{+} portion (Fig. 1 A, gate II) represented a homogenous population of MO (Fig. 1 B) that constituted 9.8 ± 0.3% of the BM and is characterized as F4/80^{hi} CD11b^{hi} CD68^{int} CX3CR1^{int} MHCII^{−} CD11c^{−} CD169^{−} (Fig. 1 C and Fig. S1 A), and will herein be termed Gr-1^{hi} MO. The Gr-1^{−}CD115^{+} population (Fig. 1 A, gate III) representing 1.4 ± 0.1% of BM consisted of a population of MO (Fig. 1 B) characterized as CX3CR1^{hi} CD11b^{int} CD68^{int} CD169^{−} and will be termed Gr-1^{lo} MO. Subsets of this population were positive for F4/80 (Fig. S1 A), CD11c, and MHC class II (Fig. 1 C).

The Gr-1^{−}CD115^{int}F4/80^{+} fraction consisted of two populations: eosinophils (Fig. 1 A, gate V) and a population of mononuclear cells (gate IV), which could be discriminated by forward and side scatter characteristics. The Gr-1^{−} CD115^{int} F4/80^{+} subset, after exclusion of SSC^{hi} eosinophils, comprised 2.6 ± 0.2% of BM cells and was the only population of BM mononuclear phagocytes that showed expression of CD169 (Fig. 1 C). CD169, also known as sialoadhesin or SIGLEC-1, is a sialic acid binding molecule that was initially described over two decades ago to have high activity on BM stromal and lymph node MΦ, but not on blood MO (Crocker and Gordon, 1986). CD169 is recognized by the MΦ antibody MOMA-1, which has long been used to stain MΦ in the spleen, lymph nodes, lamina propria, Peyer's patches, and CNS (Oetke et al., 2006). Based on this marker, we will subsequently call this cell population BM MΦ. These Gr-1^{−} CD115^{int} F4/80^{+} CD169^{+} MΦ also expressed intermediate levels of MHC class II, CD11c, and CD68; low expression of CD11b; and negligible expression of CX3CR1 (Fig. 1 C).

Depletion of BM mononuclear phagocytes correlates with HSC/progenitor egress and reduction in marrow CXCL12

We first depleted BM MO/MΦ using clodronate liposome injection. 14 h after clodronate liposome administration, BM MΦ were reduced by 84% (Fig. 2, A and B), whereas Gr-1^{hi} MO, Gr-1^{lo} MO, and total BM cellularity were reduced by 79, 88, and 24%, respectively, compared with PBS-treated animals (Fig. 2, A and C–E). Depletion of the noneosinophil Gr-1^{−} CD115^{+} F4/80^{+} population with clodronate further supports the conclusion that these CD169^{+} cells are indeed MΦ. We assessed the effect of BM MO/MΦ depletion on circulating hematopoietic progenitors and found a marked increase in colony-forming unit activity (4.5-fold; Fig. 2 F) and Lineage[−]Sca-1^{+}c-kit[+] (LSK) cells (6.2-fold; Fig. 2 G) in blood after mononuclear phagocyte depletion. Notably, circulating LSK Flk2^{−} cells, enriched in long-term repopulating HSCs (Christensen and Weissman, 2001), increased by 12.9-fold after clodronate treatment (Fig. 2 H).

We next determined the effect of mononuclear phagocyte depletion in modulating the levels of CXCL12, a chemokine produced by stromal niche cells that is crucial in retention and maintenance of HSCs/progenitors in the BM (Méndez-Ferrer and Frenette, 2007). Clodronate-induced depletion of BM MO/MΦ and HSC/progenitor mobilization was associated with a 44% reduction in CXCL12 mRNA levels in total BM (Fig. 2 I) and a 40% reduction in CXCL12 protein in the BM extracellular fluid (BMEF; Fig. 2 J). Because BM MO/MΦ do not produce CXCL12 (Fig. S2), these data suggest that MO/MΦ depletion causes a reduction in CXCL12 expression by BM stromal cells.

These results were further confirmed using other conditional depletion models of mononuclear phagocytes, including transgenic mice expressing the diphtheria toxin (DT) receptor under the CD11b promoter (CD11b-DTR;
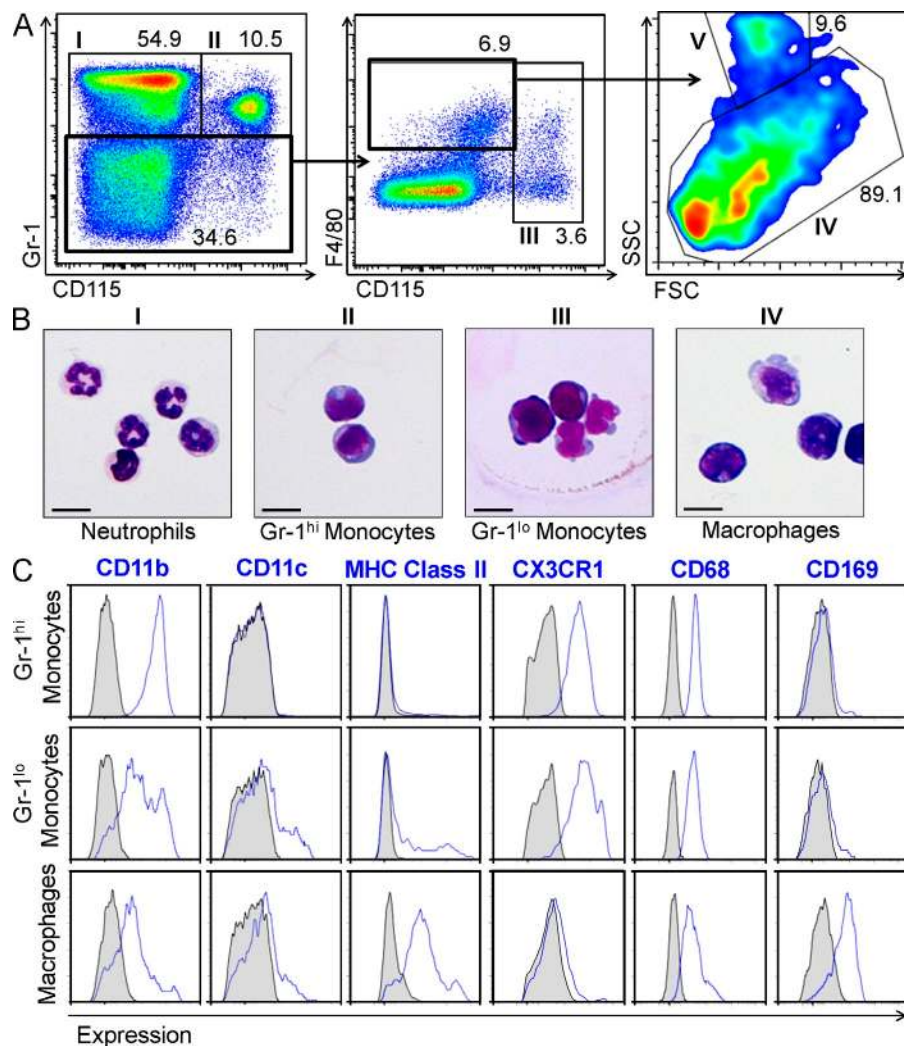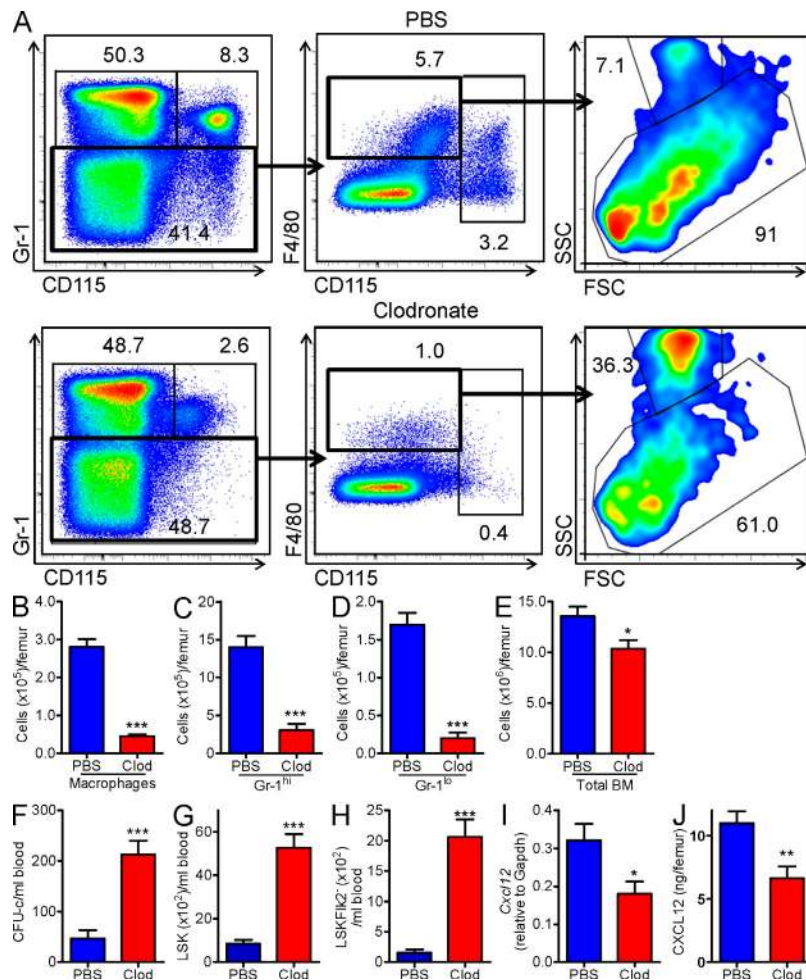
Figure 1. Mononuclear phagocytes can be distinguished in the BM with Gr–1, CD115, and F4/80. (A) Gating strategy of BM mononuclear phagocytes. The Gr-1+ populations were divided into a CD115− fraction comprised of neutrophils (I; left) and CD115+ fraction of Gr-1hi MOs (II; left). The Gr-1lo fraction was further subdivided into two populations (middle): CD115+ Gr-1lo MOs (III) and a F4/80+CD115int population, which can be subdivided into SSChi eosinophils (V) and SSCint/lo MΦ (IV). (B) Morphology of cell populations I–IV (63× magnification; bars, 10 µm). (C) Overlay histograms show the differential expression of CD11b, CD11c, MHC class II, CX3CR1, CD68, and CD169 (blue line) among mononuclear phagocyte populations. Gray histograms represent isotype control. All results are representative of two independent experiments.

47% reduction in BMEF CXCL12 (Fig. S3 S). These data are consistent with a recent study also using liposomal clodronate and Mafia mice that demonstrated the association of BM mononuclear phagocyte depletion with HSC/progenitor egress (Winkler et al., 2010). Progenitor release cannot be explained by nonspecific cell death because in vivo depletion of neutrophils and Gr-1hi MO using anti–Gr-1 (Ly6G/C) antibody or depletion of dendritic cells using DT administration in CD11c-DTR mice (Jung et al., 2002) did not lead to any progenitor mobilization (unpublished data). Collectively, these results suggest that mononuclear phagocytes play a critical role in the retention of HSCs/progenitors in the BM.

Cailhier et al., 2005) and the Mafia mice (Burnett et al., 2004). In these studies, we generated BM chimeric mice in which wild-type recipients were reconstituted with BM cells isolated from these transgenic animals to minimize toxicity of the depleting agents to nonhematopoietic organs. Treatment of CD11b-DTR chimeric animals with DT reduced BM MΦ counts by >40% (Fig. S3 A) and MO subsets by >50% (Fig. S3, B and C). Consistent with the expression of CD11b, also on neutrophils, total BM cellularity was reduced by ∼40% in this model (Fig. S3 D). Concomitantly, progenitors circulating in blood were significantly increased by ∼1.6-fold (Fig. S3 E) and BMEF CXCL12 was significantly reduced (Fig. S3 F). AP20187-treated Mafia BM chimeras depleted BM MΦ, MO, and total BM cells by 40, >80, and 30%, respectively (Fig. S3, G–J). This was associated with an ∼6-fold increase in circulating progenitors (Fig. S3 K), and 46% reduction in BM CXCL12 levels (Fig. S3 L). In nontransplanted Mafia mice, mobilization was even more robust; AP20187-treated Mafia animals exhibited a >80% reduction in MO/MΦ (Fig. S3, M–P), 31% reduction in BM cellularity (Fig. S3 Q), >20-fold increase in circulating progenitors (Fig. S3 R), and

Mononuclear phagocytes regulate Nestin+ niche cells that maintain HSCs in the BM

Recent studies have revealed that GFP expression, when driven by Nestin regulatory elements, identifies rare MSCs that form HSC niches (Méndez-Ferrer et al., 2010b). We observed CD68+ and CD169+ cells throughout the BM and in the vicinity of rare Nestin+ MSC niche cells (Fig. 3 A). To evaluate whether mononuclear phagocytes regulate Nestin+ niche cells, we used clodronate liposomes to deplete BM MO/MΦ. Because the number of Nestin+ cells was unchanged by this treatment (Fig. S4 D), we assessed alterations in gene expression in these cells. We sorted CD45− Ter119− Nestin+ and CD45− Ter119− Nestin− from the BM and CD45− Ter119− CD31− Sca-1− CD51+ osteoblasts (Semerad et al., 2005; Winkler et al., 2010) from the bone 14 h or 7 d after depletion (Fig. S4, A and B). Bone CD45− Ter119− CD31− Sca-1− CD51+ cells were confirmed to be enriched in osteoblasts by

Figure 2. Depletion of mononuclear phagocytes is associated with HSC/progenitor mobilization and CXCL12 reduction. (A–H) C57BL/6 mice were treated with PBS (blue) or clodronate-encapsulated liposomes (red). (A) Representative dot plots show the percentages of neutrophils, Gr-1^{hi} MOs, Gr-1^{lo} MOs, and MΦ, as described in Fig. 1 A. (B–E) Absolute numbers of mononuclear phagocytes and total nucleated cells in the BM ($n = 11$). (F) Absolute numbers of colony-forming units in culture in the peripheral blood (CFU-C; $n = 12$–15). (G–H) Enumeration of Lineage$^-$ Sca-1$^+$ c-kit$^+$ (LSK; G) and LSKFlk2$^-$ (H) cells in the peripheral blood ($n = 9$–10). B–H represents pooled data from at least three independent experiments. (I) RT-PCR analysis of *Cxcl12* mRNA levels in total BM cells ($n = 5$ mice per group). Data representative of two independent experiments are shown. (J) CXCL12 levels in the BMEF. Data are pooled from three independent experiments.

high *Osteocalcin* expression compared with CD45$^-$ Ter119$^-$ CD31$^+$ endothelial cells (Fig. S4 C). From these populations, we performed quantitative real-time PCR (Q-PCR) of genes encoding molecules previously implicated in HSC maintenance and retention (*Cxcl12*, *Angpt1*, *Kitl*, and *Vcam1*). These genes are highly expressed by Nestin$^+$ cells and down-regulated during G-CSF–induced mobilization or upon β3 adrenergic signaling (Méndez-Ferrer et al., 2010b). As previously reported, Nestin$^+$ cells from the BM had markedly higher expression of the four retention genes, compared with the Nestin$^-$ fraction (Méndez-Ferrer et al., 2010b). Interestingly, we found that the expression of *Cxcl12*, *Angpt1*, *Kitl*, and *Vcam1* was 48-, 18-, 65-, and 35-fold higher, respectively, in Nestin$^+$ cells in the BM compared with bone osteoblasts in the steady state (Fig. 3, B–E). Strikingly, we observed a 65–80% reduction in the expression of these four genes 14 h after treatment with clodronate, compared with PBS liposome-treated animals (Fig. 3, B–E). The reduced expression persisted at least until day 7 after treatment with clodronate (Fig. S5). In contrast, the expression levels of these retention genes in sorted osteoblasts were unchanged 14 h and 7 d after clodronate treatment. In addition, the numbers of Nestin$^+$ cells and osteoblasts 14 h and 7 d after administration of clodronate were similar to

controls (Fig. S4, D–G). These results, together with the gene expression analyses (Fig. 3, B–E; and Fig. S5), suggest that BM mononuclear phagocytes play a role in HSC/progenitor retention by regulating maintenance of retention gene expression specifically in Nestin$^+$ niche cells, but not osteoblasts.

Microarray expression analyses have shown that Nestin$^+$ cells express high levels of *Csf1* (Méndez-Ferrer et al., 2010b), a critical cytokine for MΦ development and survival (Hamilton, 2008). To determine whether Nestin$^+$ cells in the BM regulate mononuclear phagocyte numbers, we depleted Nestin$^+$ cells by administering DT into tamoxifen–treated *Nes-Cre^{ERT2}/iDTR* animals (Méndez-Ferrer et al., 2010b). We found no difference in BM MΦ (Fig. S6 A) or MO (Fig. S6, B and C) in *Nes-Cre^{ERT2}/iDTR* mice treated with tamoxifen and DT, compared with control *iDTR* animals.

BM MΦ produce a protein factor that raises CXCL12 production by stromal cells in vitro

The aforementioned results demonstrate a robust in vivo correlation between BM MO/MΦ depletion, CXCL12 reduction, and HSC/progenitor mobilization. To further dissect the effect of mononuclear phagocytes on stromal cell function, we established long-term murine Dexter BM cultures consisting of an adherent stromal layer and attached hematopoietic cells (Dexter et al., 1977). Consistent with the in vivo data, we found that clodronate liposome treatment of Dexter cultures dramatically reduced the cellularity in the wells, especially among the adherent MΦ, compared with PBS liposome-treated wells (Fig. 4 A). The number of CD115$^+$ mononuclear phagocytes was indeed reduced by >50% after liposomal clodronate treatment (Fig. 4 B). These changes in mononuclear phagocytes were associated with decreased stromal production of CXCL12 at 24 h (∼30%↓) and 72 h (∼40%↓; Fig. 4 C).
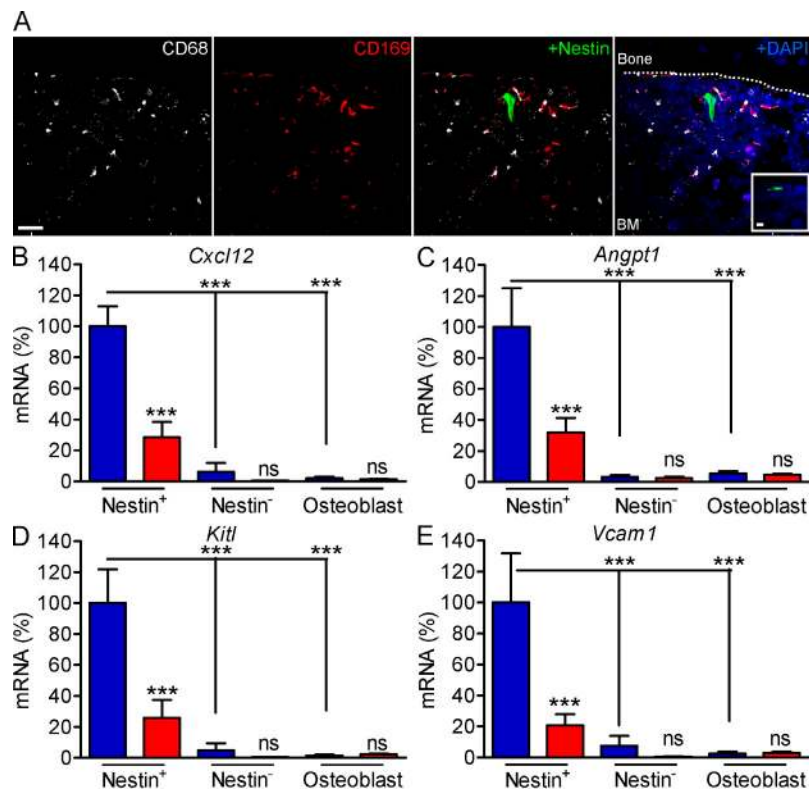
Figure 3. Anatomical and functional relationships between mononuclear phagocytes and Nestin+ niche cells. (A) Distribution of BM CD68+ (white) and CD169+ (red) cells in 5-µm femoral sections of *Nes*-GFP mice. Dashed line demarcates separation of bone and BM. Images were acquired at 40× magnification (bar, 20 µm). Isotype control is shown in inset. (B–E) Relative expression of *Cxcl12* (B), *Angpt1* (C), *Kitl* (D), and *Vcam1* (E) in CD45− Ter119− Nestin+ (Nestin+) and CD45− Ter119− Nestin (Nestin−) fractions sorted from the BM and osteoblasts sorted from the bone 14 h after treatment with PBS- (blue bars) or clodronate-encapsulated (red bars) liposomes. Data are presented with the mean expression of the PBS liposome-treated Nestin+ fraction set at 100% and are representative of three independent experiments (*n* = 4–5). Data analyzed by one-way ANOVA/Newman-Keuls test. ***, P < 0.001.

Because adherent MΦ appear to interdigitate the stroma in Dexter cultures, we sought to determine the relative contribution of MΦ and MO in stromal cell–mediated progenitor retention. Thus, we used the murine stromal cell line MS-5 to determine whether the addition of MΦ or MΦ-synthesized products could affect the stromal niche. MS-5 stromal cells have been used as an appropriate in vitro model in which to replicate in vivo modulation of CXCL12 production by noradrenergic signals (Méndez-Ferrer et al., 2008). When grown in medium conditioned by the MΦ cell line RAW264.7 (Raschke et al., 1978), CXCL12 production by MS-5 was significantly increased (Fig. S7 A), whereas no significant difference was observed in medium conditioned by the myeloid myeloblast cell line M1 (Ralph et al., 1983; Fig. S7B). Co-culture of BM-derived MΦ (BMDM) or media conditioned by BMDM increased MS-5 production of CXCL12, indicating that a secreted soluble factor induces CXCL12 up-regulation by MS-5 cells (Fig. 4, D and E). This secreted factor was a protein, as digestion with Proteinase K abrogated the ability of MΦ-conditioned medium to raise CXCL12 production by MΦ (Fig. 4 F). We have evaluated putative candidate factors using antibodies or knockout animals for IGF-1, IL-1, TNF, or IL-10. However, the loss-of-function of any one of these factors did not alter the ability of BMDM-conditioned medium to induce CXCL12 synthesis (Fig. S7, C–F). These data suggest that BM MΦ, through the secretion of a yet undefined protein factors, directly promote the retention of HSCs/progenitors by raising CXCL12 production in BM niche cells.
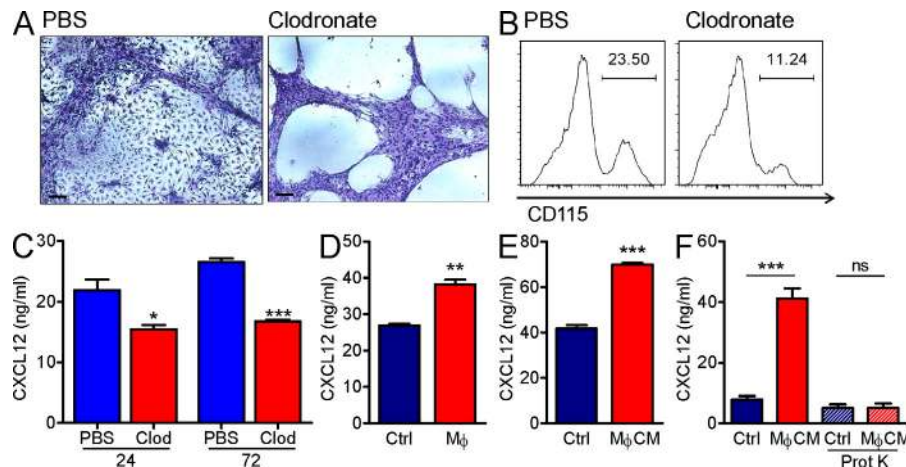
Depletion of BM CD169+ MΦ mobilizes HSCs/progenitors

The MS-5/MΦ co-culture experiments suggest that differentiated BM MΦ, rather than MO, are the mononuclear phagocytes that promote HSC/progenitor retention. To test directly whether BM MΦ are promoting HSC/progenitor retention in the BM, we took advantage of the differential expression of CD169 between MO and MΦ and mice expressing DTR under the endogenous CD169 promoter (Miyake et al., 2007). Treatment of heterozygous CD169-DTR mice with DT-depleted MΦ (Fig. 5, A and B), but not MO (Fig. 5, A, C, and D), in the BM. DT treatment was associated with a 3.5-fold increase in circulating hematopoietic progenitors, as assessed by LSK cell enumeration (Fig. 5 E), and a 5.4-fold increase in the stem cell-enriched LSKFlk2− fraction (Fig. 5 F). Moreover, depletion of CD169+ MΦ from long-term Dexter culture resulted in a 42% reduction in the ability of BM stromal cells to produce CXCL12 (Fig. 5 G). Thus, CD169+ MΦ in the BM promote stromal production of CXCL12, and their specific depletion in vivo is sufficient to mobilize HSCs/progenitors.

Parallel and antagonistic roles of MΦ and SNS in regulating HSC/progenitor release

The SNS is crucial in HSC/progenitor trafficking (Katayama et al., 2006; Méndez-Ferrer et al., 2008) where β3-adrenergic receptor (β3R) signaling plays a key role in circadian oscillations of HSC release, and both β2-adrenergic receptor (β2R) and β3R signaling cooperate in G-CSF–enforced egress (Méndez-Ferrer et al., 2010a). MΦ could act independently, or alternatively, through alterations in the sympathetic tone. Thus, to assess whether MΦ operate through a distinct pathway, we examined whether clodronate treatment was capable of inducing mobilization in sympathectomized animals. We found that mice chemically sympathectomized with 6-hydroxydopamine (6OHDA) still exhibited significant progenitor mobilization (>7-fold) in response to clodronate

Figure 4. MΦ in culture promote CXCL12 production. (A) Morphology of adherent layer of Dexter culture 24 h after addition of PBS or clodronate liposomes (10×; bars, 100 μm). (B) Adherent cells were analyzed by flow cytometry for CD115+ cells. (A and B) Representative data from two independent experiments are shown. (C) CXCL12 levels were assessed by ELISA at 24 h (left bars) and 72 h (right bars) after liposomal incubation. (D) CXCL12 levels were assessed 3 d after MS-5 cells were co-cultured with (MΦ) or without (Ctrl) BMDM. (E) Levels of CXCL12 secreted from MS-5 cells after culture with medium conditioned by BMDM (MΦ CM) or with control medium (Ctrl). (F) CXCL12 levels were measured after culture of MS-5 cells with control (Ctrl, blue) or MΦ-conditioned (MΦ CM, red) medium that was untreated (left two bars) or treated with Proteinase K (right two bars). (C–F) Representative data from at least two independent experiments are shown.

treatment; however, the absolute number of mobilized progenitors did not reach the level of SNS–intact Clodronate-treated mice (Fig. 6 A, mid-left bars). To evaluate this issue using another model, we used mice deficient in β2R (*Adrb2⁻/⁻*) treated with an antagonist to the β3R. Clodronate treatment was still able to cause HSC/progenitor mobilization (>3-fold) in these mice, but again HSCs/progenitors did not mobilize to the same level as wild type animals (Fig. 6 A, mid-right bars). To dissect further the relative contribution of the β2R and β3R in SNS promotion of HSC/progenitor release, we evaluated the effect of MΦ depletion in mice singly lacking β2R (Fig. 6 A, right bars) or β3R (Fig. 6 B). Whereas clodronate treatment led to a robust increase in circulating progenitors in *Adrb2⁻/⁻* animals compared with wild-type animals (Fig. 6 A, right bars), the response was blunted in *Adrb3⁻/⁻* mice (Fig. 6 B). These data are consistent with previous studies demonstrating that β3R, but not β2R, signaling is critical for physiological HSC/progenitor release (Méndez-Ferrer et al., 2008). The fact that MΦ depletion can still mobilize HSCs—albeit at lower amplitude—when SNS signaling is disrupted, argues that the SNS and the BM MΦ act through distinct parallel pathways. Thus, these data suggest antagonistic functions of the autonomic nervous system and innate immunity in regulating the niche (Fig. 6 C), where the SNS promotes egress by reducing the expression of key retention factors by the niche cell (Méndez-Ferrer et al., 2010b), and in contrast, BM MΦ promotes the expression of these genes and HSC/progenitor retention in the BM.

BM MΦ depletion synergizes with enforced HSC/progenitor mobilization

Because the expression of retention genes is still reduced in the Nestin+ niche cells 7 d after clodronate treatment (Fig. S5), we sought to determine the duration of MΦ reduction and the kinetics of recovery. We found that BM MΦ remain markedly (>90%) reduced 10 d after clodronate treatment (Fig. 7 A). Recovery started by day 16 (58% reduction) and clodronate-treated mice demonstrated no reduction in MΦ counts by day 28. Alternatively, MO populations in the BM

began their recovery by day 7 after clodronate administration (unpublished data). Interestingly, levels of LSK (Fig. 7 B) and LSKFlk2⁻ (Fig. 7 C) inversely matched BM MΦ counts. HSCs/progenitors were still elevated in the circulation 10 d after clodronate administration (4.2- and 3.2-fold, respectively), and mobilization persisted at least until day 16 (Fig. 7 C). These data further support the specific role of BM MΦ, but not MO, in promoting the retention of HSCs/progenitors in the BM.

Because BM MΦ promote HSC/progenitor retention, we examined whether elimination of this population would enhance mobilization using the CXCR4 antagonist AMD3100 or G-CSF, both of which are clinically approved mobilizing agents. We found that clodronate treatment 14 h before harvest doubled HSC/progenitor mobilization in AMD3100-treated animals and resulted in a significant increase in the number of HSCs/progenitors mobilized by G-CSF (Fig. 7, D–E). To further assess the role of MΦ in a situation where progenitor mobilization is suboptimal, we treated mice with G-CSF (Hidalgo et al., 2004) for 2 d, instead of 4 d. We found that CFU-C, LSK, and LSKFlk2⁻ cells in the peripheral blood mobilized by 2 d of G-CSF were increased 3.8-, 5.9-, and 9.3-fold (Fig. 7, F–H), respectively, in mice that were treated with clodronate liposomes 14 h before harvest. Furthermore, we tested whether depleting MΦ 10 d before blood collection, rather than 14 h before collection, could synergize with 4 d G-CSF treatment. Indeed, when mice were preinfused with clodronate liposomes 10 d before harvest, they had 5.2-, 3.4-, 2.7- fold higher CFU-C, LSK, and LSKFlk2⁻ in the peripheral blood, respectively (Fig. 7, I, J, K). Thus, targeting BM MΦ may be a novel modality by which to enhance mobilization yields in patients.

DISCUSSION

In this study, we sought to identify the role of BM mononuclear phagocytes in HSC/progenitor mobilization. Unexpectedly, we found that depletion of mononuclear phagocytes
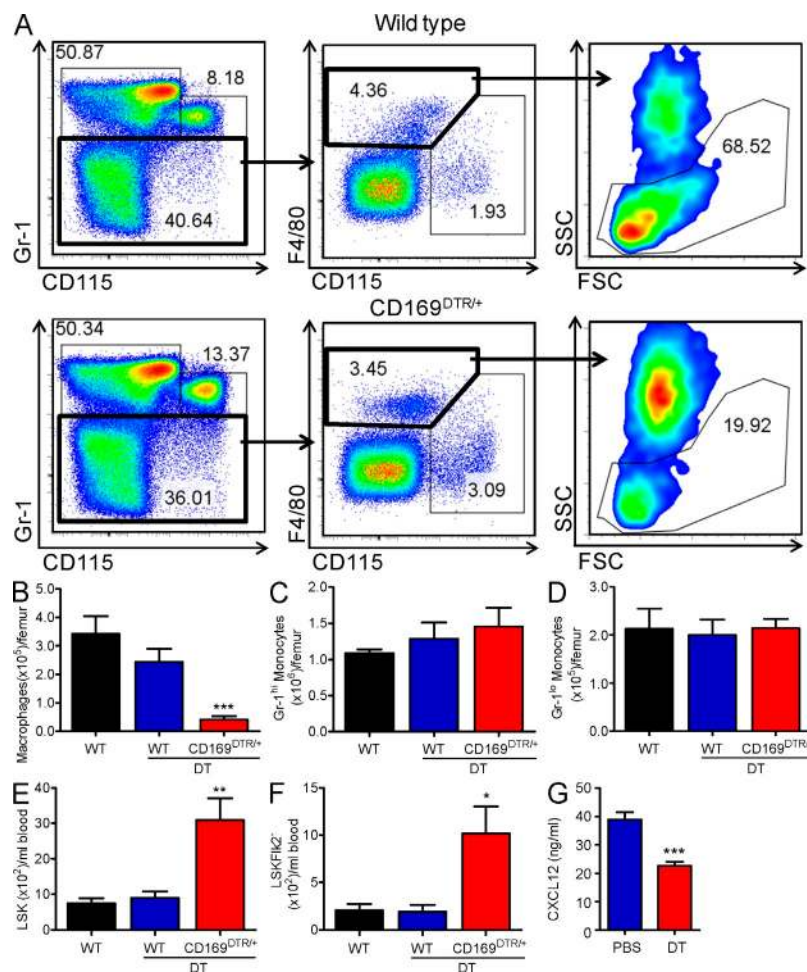
Figure 5. Depletion of BM CD169⁺ MΦ, but not CD169⁻ MOs, mobilizes HSCs/progenitors.

(A–D) Wild-type (WT) or heterozygous CD169-DTR (CD169^DTR/+) mice were treated with DT. (A) Representative dot plots show the percentages of BM mononuclear phagocytes in wild-type (top) or CD169^DTR/+ mice treated with DT (bottom). (B–D) Bar graphs depict the absolute numbers of mononuclear phagocytes (*n* = 6) in wild type mice and wild type or CD169^DTR/+ mice injected with DT. (E–F) Bar graphs enumerate Lineage⁻ Sca-1⁺ c-kit⁺ (LSK; E) and LSKFlk2⁻ cells (F) per milliliter of blood in the same mice analyzed in B–D (*n* = 6). Data are pooled from two independent experiments. (G) CXCL12 levels were measured 72 h after administration of PBS or 1 μg/ml DT into Dexter cultures plated from the BM of CD169-DTR animals (*n* = 3–4 wells). Representative data from two independent experiments are shown.

of niche cells that express Nestin (Méndez-Ferrer et al., 2010b).

Although osteoblasts have been proposed to represent a HSC niche, selective modulation of osteoblast numbers do not necessarily alter HSC numbers (Wilson and Trumpp, 2006; Kiel et al., 2007; Zhu et al., 2007), and the lack of osteoblasts in sites of extramedullary hematopoiesis suggest that they are dispensable to support HSCs. Recent studies have suggested that a more primitive precursor of osteoblasts compose the stem cell niche (Méndez-Ferrer et al., 2010b; Omatsu et al., 2010). Steady-state Nestin⁺ MSCs express substantially higher levels of genes required in HSC/progenitor maintenance and retention, including *Cxcl12*, compared with in vivo sorted (Fig. 3 and Fig. S5) or cultured osteoblasts (Méndez-Ferrer et al., 2010b). The relatively low expression of *Cxcl12* detected in sorted osteoblasts is consistent with a recent study showing that DT administration into *Cxcl12*-DTR–GFP mice did not result in loss of spindle-shaped N-cadherin–expressing osteoblasts (Omatsu et al., 2010). It has been proposed that MΦ depletion mobilizes HSCs/progenitors by disruption of the
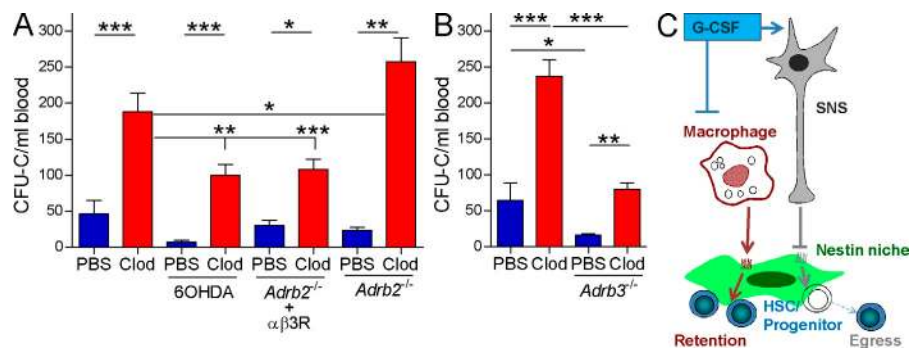
using four in vivo models was sufficient to mobilize HSCs/progenitors. Before this study, mononuclear phagocytes in the BM had been poorly characterized and relied on F4/80, a marker with a promiscuous expression profile in the BM (Fig. S1). Herein, we rigorously discriminated among Gr-1^hi MOs, Gr1^lo MOs, and MΦ in the BM by differential expression of Gr-1, CD115, F4/80, CD11b, CD11c, MHC class II, CX3CR1, CD68, and CD169. Using CD169^DTR/+ animals, we were able to implicate MΦ, constituting ∼2.6% of total BM cells, in the promotion of HSC/progenitor retention through interaction with the recently characterized population

Figure 6. Opposite influences of the MΦ and the SNS on HSC/progenitor retention.

(A) CFU-C after treatment with PBS (blue bars) or clodronate liposomes (red bars) in wild-type C57BL/6 (*n* = 11–13), 6OHDA-treated mice (*n* = 12–13), β2-adrenergic receptor–deficient (*Adrb2⁻/⁻*) mice treated with an antagonist to the β3-adrenergic receptor (αβ3R; *n* = 10), and *Adrb2⁻/⁻* mice (*n* =7). Data are pooled from three independent experiments and analyzed with one-way ANOVA/Newman-Keuls test. (B) CFU-C after treatment with PBS (blue bars) or clodronate (red bars) in wild-type FVB mice (*n* = 5) and β3-adrenergic receptor-deficient (*Adrb3⁻/⁻*) mice (*n* = 8). Data are pooled from two independent experiments. (C) Schematic of antagonistic regulation of HSC/progenitor retention by MΦ and the SNS.
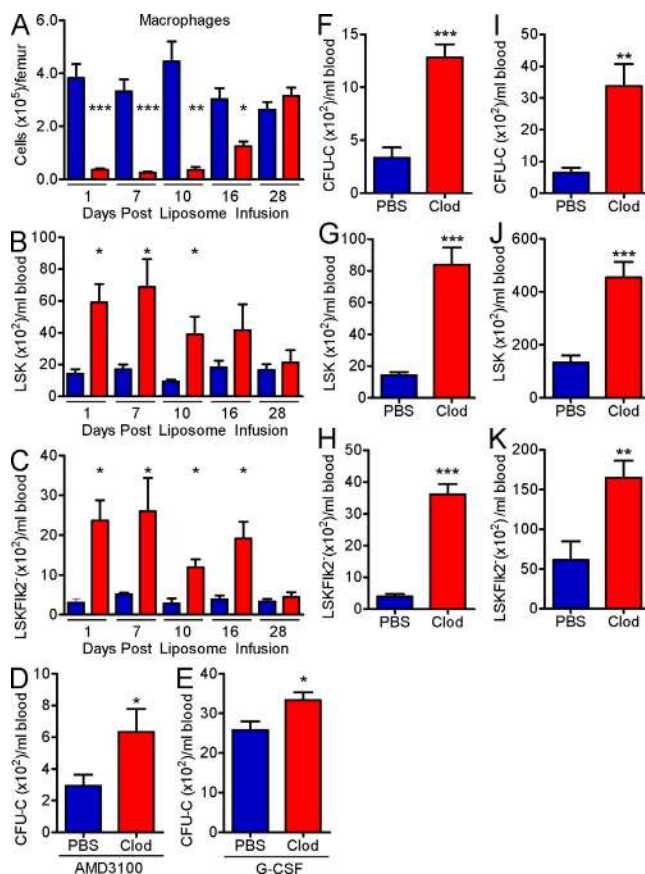
Figure 7. MΦ depletion synergizes with AMD3100 and G-CSF mobilization. (A–C) Kinetics of MΦ reduction (A) and LSK (B) and LSKFlk2⁻ (C) mobilization, at the indicated time points, after administration of PBS- (blue) or clodronate-encapsulated (red) liposomes ($n = 3$–4). Data are pooled from two independent experiments. (D–E) CFU-C from peripheral blood of mice that were treated with PBS (blue) or clodronate liposomes (red; 14 h before harvest) and mobilized with AMD3100 (D; 1 h before harvest) or G-CSF (E; 4 d). Data are pooled from two independent experiments. (F–H) CFU-C (F), LSK (G), and LSKFlk2⁻ (H) cells from the peripheral blood of mice that were mobilized for 2 d with G-CSF and treated with PBS- or clodronate-encapsulated liposomes 14 h before harvest. Experiment was performed once ($n = 4$). (I–K) CFU-C (I), LSK (J), and LSKFlk2⁻ (K) from 16-wk-old female mice that were pretreated with PBS- or clodronate-encapsulated liposomes 10 d before harvest and mobilized with G-CSF for 4 d. Data are representative of two independent experiments ($n = 4$).

osteoblastic niche (Winkler et al., 2010). Winkler et al. observed a reduction in osteoblast numbers, as determined by histomorphometry, on day 4 after two treatments with clodronate liposomes on days 0 and 2. Although we have not observed any significant reduction in osteoblast counts 14 h or 7 d after clodronate treatment, it remains possible that osteoblast numbers may have transiently decreased and recovered after MΦ ablation. In addition to CXCL12, the regulation of other key retention genes appears to correlate with HSC/progenitor egress. For example, treatment with G-CSF or β3R agonists down-regulates *Cxcl12*, *Angiopoietin-1*, *Kitl*, and *Vcam-1* (Méndez-Ferrer et al., 2010b). We have not detected any reductions in the expression of HSC retention genes in

osteoblasts either 14 h or 7 d after the depletion of MΦ, despite the fact that HSCs/progenitors were clearly elevated at both time points. In contrast, significant reductions in the expression of HSC retention genes were observed in Nestin⁺ cells, and correlated with persistent HSC/progenitor mobilization even 7 d after clodronate treatment. These results thus indicate that CD169⁺ BM MΦ promote HSC retention by acting specifically on the Nestin⁺ HSC niche in the BM.

Previous studies have revealed that a transplantable cell expressing the G-CSF receptor (G-CSFR) is essential for G-CSF–induced mobilization (Liu et al., 2000). An accompanying study, using an elegant mouse model in which the G-CSFR is expressed exclusively in CD68-expressing cells, also implicates mononuclear phagocytes in G-CSF mobilization (see Christopher et al. in this issue). Thus, G-CSF signaling exclusively in MΦ is sufficient to reduce niche retention and promote HSC/progenitor mobilization. However, because G-CSF–induced HSC/progenitor mobilization is at least three times more potent than MΦ depletion with clodronate liposomes (this study; Winkler et al., 2010), it must also be acting on cells other than MΦ.

The SNS is required for progenitor egress (Katayama et al., 2006; Méndez-Ferrer et al., 2010a), suggesting that G-CSF–mediated increase of sympathetic tone in the BM may represent a putative MΦ-independent target. Our results using models with impaired sympathetic activity suggest that BM MΦ exert antagonistic, independent regulatory functions in the HSC niche compared with the SNS. Although G-CSF likely has several targets in the BM microenvironment, the present data uncover two distinct opposing activities that lead to major changes in HSC retention by Nestin⁺ niche cells. We thus propose that G-CSF induces HSC mobilization by inhibiting MΦ-mediated retention signals and simultaneously enhancing sympathetic-mediated progenitor release (Fig. 6 C).

These results expand our understanding of HSC niche components by implicating a cellular constituent of the innate immune system, the CD169⁺ MΦ, as a niche regulator. Because targeted reduction of BM MΦ can enhance HSC/progenitor mobilization, the use of antibodies against CSF-1 (M-CSF), its receptor, or small molecule inhibitors of M-CSF signaling may provide a novel strategy to increase the efficiency of HSC/progenitor mobilization for autologous transplantation.

MATERIALS AND METHODS

Mice. All experiments, unless otherwise noted, were performed on 8–10-wk-old C57BL/6 male mice from Charles River Laboratories (Frederick Cancer Research Center, Frederick, Maryland). β2-adrenergic receptor-deficient (*Adrb2^tm1Bkk*/J; Chruscinski et al., 1999; gift from G. Karsenty, Columbia University, New York, NY), β3-adrenergic receptor-deficient (FVB/N-*Adrb3^tm1low*l/J; Susulic et al., 1995; The Jackson Laboratory), FVB/N-CD11b-DTR (Cailhier et al., 2005; gift from C. Aloman, Mount Sinai Medical Center, New York, NY), Mafia (C57BL/6-Tg[Csf1r-EGFP-NGFR/FKBP1A/TNFRSF6]2Bck/J; Burnett et al., 2004; The Jackson Laboratory), CX3CR1/GFP (Jung et al., 2000; gift from D. Littman, New York University, New York, NY), CD169-DTR (Miyake et al., 2007), *Nes-Gfp* (Mignone et al., 2004), *Nes-Cre^ERT2* (Balordi and Fishell, 2007), *iDTR* (C57BL/6-Gt[R OSA]26Sortm1[HBEGF]Awai/J; Buch et al., 2005), IL-10⁻/⁻ (Berg et al., 1996;

gift from H. Xiong, Mount Sinai Medical Center, New York, NY), and TNF$^{-/-}$ (Marino et al., 1997; gift from M. van den Brink, Memorial Sloan Kettering Cancer Center, New York, NY) mice were also used in these studies. FVB/N-CD11b-DTR and Mafia (CD45.2) BM chimeras were generated by transplanting 2.0×10^6 and 1.9×10^6 BM-nucleated cells from male donors into lethally irradiated 8-wk-old FVB/N (The Jackson Laboratory) and C57BL/6 Ly5.2 (CD45.1) male mice, respectively. BM and blood of Mafia BM chimeras showed >95% donor chimerism as assessed by flow cytometry 1 mo after transplantation. Mice were maintained on a 12 h light/12 h darkness lighting schedule. All in vivo experiments were harvested between 12:00 and 1:00 p.m. (Zeitgeber time 5:00 and 6:00) to limit circadian variations in HSC/progenitor release (Méndez-Ferrer et al., 2008) and mobilization (Lucas et al., 2008). All mice were housed in specific pathogen–free facilities at the Mount Sinai School of Medicine or Albert Einstein College of Medicine animal facility. Experimental procedures performed on the mice were approved by the Animal Care and Use Committee of the Mount Sinai School of Medicine and Albert Einstein College of Medicine.

In vivo cell depletion. Cl2MDP (or clodronate) was a gift from Roche (Van Rooijen and Sanders, 1994). Clodronate liposomes (250 µl) were infused i.v. at 1 d (14 h), 7 d, 10 d, 16 d, or 28 d before harvest. CD11b-DTR mice were treated with DT i.p. 25 ng/g on days 1 and 3 before harvest. DT was purchased from Sigma-Aldrich. AP20187 was a gift from Ariad Pharmaceuticals. Lyophilized AP20187 was dissolved in 100% ethanol at a concentration of 62.5 mg/ml stock solution and was stored at −20°C. As recommended by Ariad Pharmaceuticals, injection solutions were prepared with a diluent composed of 4% ethanol, 10% PEG-400, and 2% Tween-20 in water. All injections were administered i.v. within 30 min after preparation. The volume of injection solution was adjusted according to the average mouse body weight to deliver a dose of 10 mg/kg AP20187 per mouse in an mean volume of 100 µl. Mice were injected daily for 5 d before harvest. Heterozygous CD169-DTR (CD169$^{DTR/+}$) or control C57BL/6 were injected i.p. with 10 µg/kg DT 48 h before harvest. Depletion of Nestin$^+$ cells was accomplished as previously described (Méndez-Ferrer et al., 2010b).

Flow cytometry and cell sorting. Fluorochrome-conjugated or biotinylated mAbs specific to mouse Gr-1 (Ly6G/C; clone RB6-8C5), CD115 (clone AFS98), Siglec-F (clone E50-2440), CD11b (clone M1/70), CD11c (clone N418), I-A/I-E clone (clone M5/114.15.2), CD45 (clone 30-F11), Sca-1 (clone D7), Flk2 (clone A2F10), CD117 (clone 2B8), CD3 (clone 145-2C11), B220 (clone RA3-6B2), Ter119 (clone TER-119), CD51 (clone RMV-7), and CD31 (clone MEC13.3), corresponding isotype controls, and secondary reagents (efluor450-, APC-efluor780–, and PE-Cy7–conjugated streptavidin) were purchased from eBioscience. Anti-F4/80 (clone CI:A3.1), CD68 (clone FA-11), and CD169 (clone 3D6.112) were purchased from AbD Serotec. CD68 was stained extracellularly and subsequently intracellularly with the Cytofix/Cytoperm kit (BD) according to the manufacturer's protocol. Multiparameter analyses of stained cell suspensions were performed on an LSRII (BD) and analyzed with FlowJo software (Tree Star, Inc.). DAPI$^-$ single cells were evaluated for all analyses except for intracellular stains. To purify mononuclear phagocyte populations, BM was sorted with an InFlux cell sorter (BD) to achieve >97% purity. Sorted mononuclear phagocytes were cytospun with Cytospin 3 (Thermo Fisher Scientific) and stained with Hema 3 manual staining system (Thermo Fisher Scientific). To isolate Nestin$^+$ and Nestin$^-$ cells from the BM for Q-PCR, RBC-lysed BM cells were digested with collagenase, trypsin, and DNase, as previously described (Méndez-Ferrer et al., 2010b). Endothelial cells and osteoblasts were isolated similar to previous studies (Semerad et al., 2005; Winkler et al., 2010). In brief, tibias, femurs, and humeri of mice were flushed thoroughly of BM cells, chopped with a scalpel, and washed three times through a 5-ml polystyrene tube with blue-top cell strainer (BD) to further remove residual BM cells. The bone fragments were then digested at 37°C with Type IA collagenase (Sigma-Aldrich) for 40 min while spinning. RBC-lysed pellet was then stained for sorting. Cells were sorted by Moflo Cell sorter (Dako) at the Flow Cytometry Core Facility at Mount Sinai School of Medicine or Aria Cell sorter (BD) at the Flow Cytometry Core Facility at Albert Einstein College of Medicine.

CFU-C assays and mobilization. Colony-forming assays were performed as previously described (Frenette et al., 1998). Mobilization experiments with AMD3100 and 4-d G-CSF were performed as previously described (Katayama et al., 2006; Lucas et al., 2008). Some experiments were performed with suboptimal G-CSF treatment (2 d), as previously described (Hidalgo et al., 2004).

RNA isolation, reverse transcription, and Q-PCR. For measurement of BM *Cxcl12* gene expression, femurs were flushed and mixed with 0.5 ml Trizol (Invitrogen) and stored at −80°C. Conventional reverse transcription, using the Sprint PowerScript reverse transcription (Takara Bio Inc.) was performed in accordance with the manufacturer's instructions. Q-PCR was performed with SYBR GREEN on an ABI PRISM 7900HT Sequence Detection System (Applied Biosystems). The PCR protocol consisted of one cycle at 95°C (10 min) followed by 40 cycles of 95°C (15 s) and 60°C (1 min). Expression of *Gapdh* was used as a standard. The mean threshold cycle number (C_t) for each tested mRNA was used to quantify the relative expression of each gene: 2^(C_t[*Gapdh*] − C_t[gene]). Primers used are listed below: Cxcl12_fwd, 5′-CGCCAAGGTCGTCGCCG-3′; Cxcl12_rev, 5′-TTGGCTCTGGCGATGTGGC-3′; Angpt1_fwd, 5′-CTCGTCAG-ACATTCATCATCCAG-3′; Angpt1_rev, 5′-CACCTTCTTTAGTG-CAAAGGCT-3′; Kitl_fwd, 5′-CCCTGAAGACTCGGGCCTA-3′; Kitl_rev, 5′-CAATTACAAGCGAAATGAGAGCC-3′; Vcam1_fwd, 5′-GACC-TGTTCCAGCGAGGGTCTA-3′; Vcam1_rev, 5′-CTTCCATCCT-CATAGCAATTAAGGTG-3′; Osteocalcin_fwd, 5′-GGGCAATAAGG-TAGTGAACAG-3′; Osteocalcin_rev, 5′-GCAGCACAGGTCCTAAA-TAGT-3′; Gapdh_fwd, 5′-TGTGTCCGTCGTGGATCTGA-3′; Gapdh_rev, 5′-CCTGCTTCACCACCTTCTTGA-3′.

CXCL12 ELISA. 96-well ELISA plates were coated overnight at 4°C with 50 µl of 2 µg/ml anti-CXCL12 coating antibody (MAB350; R&D Systems). Next, the wells were washed three times with wash buffer (0.05% Tween 20 in PBS) and incubated for 1 h at room temperature with 200 µl of blocking buffer (1% BSA, 5% D-Sucrose, and 0.05% NaN$_3$ in PBS; all from Thermo Fisher Scientific). After 3 washes, 100 µl of samples diluted 1:2 in PBS were added and incubated for 2 h at room temperature. After 3 washes, 100 µl of 0.250 µg/ml polyclonal biotinylated anti–human/mouse SDF-1 (BAF310; R&D Systems) was added and incubated for 2 h at room temperature. After 3 washes, 100 µl of 0.1 µg/ml Neutravidin-HRP (Thermo Fisher Scientific) was added and incubated for 30 min. After 3 additional washes, the reaction was developed by incubation for 20–30 min with 50 µl of TMB substrate solution (Sigma-Aldrich) and stopped by adding 50 µl of 1M HCl solution (Thermo Fisher Scientific). Optical density was determined with a microplate reader set at 450 nm. Optical density of PBS control wells was subtracted from optical density of samples. Recombinant mSDF-1α (PeproTech) was used to generate a linear standard curve.

Immunofluorescence. Anesthetized *Nes*-GFP transgenic animals (Mignone et al., 2004) were perfused, and femurs and tibia were sectioned and stored as previously described (Méndez-Ferrer et al., 2008). Slides were washed three times in Coplin jars (Sigma-Aldrich) to remove OCT solution residue, and then incubated for 1 h at room temperature in 20% goat serum (Sgma-Aldrich) diluted in PBS + 0.1% Tween solution (PBSTw). After 3 washes in PBSTw, slides were incubated in PBSTw + 2% goat serum + 0.5% Triton X-100 for 1 h at room temperature. After 3 washes in PBSTw, slides were incubated in primary antibody (anti-CD68-Alexa Fluor 647 [clone FA-11; AbD Serotec] and anti–CD169-biotin [clone MOMA-1; AbCam]) at a 1:100 concentration in PBSTw + 2% goat serum overnight in the dark at room temperature. After three washes in PBSTw, CD169 staining was continued with streptavidin–PE staining for 5 min. Slides were mounted with Vectorshield + DAPI, covered, and sealed with nail polish. Images were acquired on an Examiner microscope (Carl Zeiss, Inc.) and all images were processed using Slidebook software (Intelligent Imaging Innovations, Inc).

Long-term BM Dexter cultures. 3.7×10^6 BM-nucleated cells were plated in 1 ml Dexter medium (Myelocult M5300 media [Stem Cell Technologies] supplemented with 1% penicillin–streptomycin [Cellgro],

1% amphotericin [Cellgro], and 10^{-6} M freshly thawed Hydrocortisone [Sigma-Aldrich]) in 12-well plates. Cultures were maintained in a water-jacketed incubator at 33°C and 5% CO_2. Half the media was changed weekly for 6 wk. In the sixth week, the culture media was removed and replaced with 1 ml of Dexter medium containing 40% PBS- or clodronate-encapsulated liposomes by volume in some experiments. After 24-h incubation, the culture media was removed and 1 ml fresh media was added. 24 h and 72 h later, the media was collected and frozen to assess CXCL12 levels by ELISA and the adherent layer was Hema 3-stained to assess cell morphology or detached by cell scraper (BD) for flow cytometric analysis. In experiments with Dexter cultures derived from CD169$^{DTR/+}$ BM, the media was removed and replaced with 1 ml fresh Dexter medium containing PBS or 1 µg/ml DT. After 72 h of incubation, the media was frozen and later assessed for CXCL12 levels by ELISA.

MS-5 cell culture. MS-5 cells were grown in monolayers in complete medium (α–MEM medium supplemented with 10% FBS [Stem Cell Technologies], penicillin–streptomycin [Invitrogen], 5% glutamine [Invitrogen], and 5% sodium pyruvate [Invitrogen]). Cultures were maintained at 37°C and 1:10 split with 0.05% trypsin-EDTA (Invitrogen) every 3 or 4 d, when cells reached ∼80% confluence. 5,000 MS-5 cells were plated in 300 µl complete medium in 48-well plates for 24 h before addition of BMDM or medium conditioned by BMDM (MΦ CM), RAW264.7, or M1 cells (see below).

BM MO/MΦ cell culture. The M1 myeloblast cell line was cultured in DME medium (Cellgro) supplemented with 10% FBS, 2 mM L-glutamine (Sigma-Aldrich), 1% sodium pyruvate (Invitrogen), and 1% penicillin-streptomycin. RAW264.7 MΦ cell line (a gift from B. Tenoever, Mount Sinai Medical Center, New York, NY) was cultured identically to the M1 myeloblast cell line, except for addition of 100 mM Hepes (Sigma-Aldrich). 50,000 RAW264.7 and M1 cells were plated in 300 µl in a 48-well plate. 3 d later, the supernatant was collected, centrifuged at 15 g for 5 min at 4°C to remove cellular debris, mixed with MS-5 complete media at 25 or 50% concentration, and added to MS-5 cells (see previous paragraph). BMDM were derived by plating 10,000 total BM-nucleated cells in 300 µl of complete medium with 25% conditioned medium from the sarcoma cell line MS-180 (Rosenthal et al., 1990). The MS-180–conditioned medium was observed to generate MΦ robustly. The majority of the cells were adherent at day 5, displayed elongated processes consistent with MΦ morphology, and >95% were F4/80$^+$ CD115$^+$ in staining by flow cytometry. In some experiments, BMDMs were derived from $Tnfa^{-/-}$ and $Il10^{-/-}$ animals. In some experiments, IL-1 receptor antagonist (R&D Systems), or antibody against IL-1R, or IGF-1 (R&D) were added into MS5 culture with MΦ CM. All cells were grown at 37°C and 5% CO_2.

Proteinase K digestion of MΦ CM. MΦ CM was treated with 0.5 mg/ml proteinase K (Sigma-Aldrich, St. Louis, MO) for 30 min at 37°C and then heat inactivated at 95°C for 10 min. Heat-inactivated FBS was re-added to MΦ CM to the 10% concentration of the native media.

Sympathectomy. Chemical sympathectomy was performed by i.p. injection of 100 mg/kg and 250 mg/kg of 6OHDA (Sigma-Aldrich) dissolved in PBS solution containing 200 mg/kg and 500 mg/kg ascorbic acid (Sigma-Aldrich) on day −4 and −2, respectively, before harvest. Pan-adrenergic receptor abrogation was accomplished by injecting $Adbr2^{tm1Bkk}$/J (Chruscinski et al., 1999) animals with 2.5–5 mg/kg of β3-adrenergic receptor antagonist (SR59230A, i.p.; Sigma-Aldrich).

Statistical analyses. Unless otherwise indicated, the unpaired Student's t test was used in all analyses, data in bar graphs are represented as mean ± SEM, and statistical significance was expressed as follows: *, P < 0.05; **, P < 0.01; ***, P < 0.001; ns, not significant

Online supplemental material. Fig. S1 shows that BM neutrophils, MOs, and eosinophils express F4/80. Fig. S2 shows that MΦ do not produce CXCL12. Fig. S3 shows three other models in which mononuclear phagocyte depletion is associated with robust HSC/progenitor mobilization and

CXCL12 reduction. Fig. S4 shows the sorting strategy for Nestin$^+$ and Nestin$^-$ fractions and bone endothelial cell and osteoblast fractions. Fig. S5 shows that retention gene expression is reduced in Nestin$^+$ cells seven days after mononuclear phagocyte treatment. Fig. S6 shows that mononuclear phagocytes are not reduced 7 d after depletion of Nestin$^+$ cells. Fig. S7 shows that soluble factor from a MΦ, but not myeloblast, cell line enhances stromal CXCL12 production. Online supplemental material is available at http://www.jem.org/cgi/content/full/jem.20101688/DC1.

REFERENCES

Balordi, F., and G. Fishell. 2007. Mosaic removal of hedgehog signaling in the adult SVZ reveals that the residual wild-type stem cells have a limited capacity for self-renewal. *J. Neurosci.* 27:14248–14259. doi:10.1523/JNEUROSCI.4531-07.2007

Bensinger, W., J.F. DiPersio, and J.M. McCarty. 2009. Improving stem cell mobilization strategies: future directions. *Bone Marrow Transplant.* 43:181–195. doi:10.1038/bmt.2008.410

Berg, D.J., N. Davidson, R. Kuhn, W. Muller, S. Menon, G. Holland, L. Thompson-Snipes, M.W. Leach, and D. Rennick. 1996. Enterocolitis and colon cancer in interleukin-10-deficient mice are associated with aberrant cytokine production and CD4(+) TH1-like responses. *J. Clin. Invest.* 98:1010–1020. doi:10.1172/JCI118861

Buch, T., F.L. Heppner, C. Tertilt, T.J. Heinen, M. Kremer, F.T. Wunderlich, S. Jung, and A. Waisman. 2005. A Cre-inducible diphtheria toxin receptor mediates cell lineage ablation after toxin administration. *Nat. Methods.* 2:419–426. doi:10.1038/nmeth762

Burnett, S.H., E.J. Kershen, J. Zhang, L. Zeng, S.C. Straley, A.M. Kaplan, and D.A. Cohen. 2004. Conditional macrophage ablation in transgenic mice expressing a Fas-based suicide gene. *J. Leukoc. Biol.* 75:612–623. doi:10.1189/jlb.0903442

Cailhier, J.F., M. Partolina, S. Vuthoori, S. Wu, K. Ko, S. Watson, J. Savill, J. Hughes, and R.A. Lang. 2005. Conditional macrophage ablation demonstrates that resident macrophages initiate acute peritoneal inflammation. *J. Immunol.* 174:2336–2342.

Chang, M.K., L.J. Raggatt, K.A. Alexander, J.S. Kuliwaba, N.L. Fazzalari, K. Schroder, E.R. Maylin, V.M. Ripoll, D.A. Hume, and A.R. Pettit. 2008. Osteal tissue macrophages are intercalated throughout human and mouse bone lining tissues and regulate osteoblast function in vitro and in vivo. *J. Immunol.* 181:1232–1244.

Christensen, J.L., and I.L. Weissman. 2001. Flk-2 is a marker in hematopoietic stem cell differentiation: a simple method to isolate long-term stem cells. *Proc. Natl. Acad. Sci. USA.* 98:14541–14546. doi:10.1073/pnas.261562798

Christopher, M.J., M. Rao, F. Liu, J.R. Woloszynek, and D.C. Link. 2011. Expression of the G-CSF receptor in monocytic cells is sufficient to mediate hematopoietic progenitor mobilization by G-CSF in mice. *J. Exp. Med.* 208:■■■–■■■.

Chruscinski, A.J., D.K. Rohrer, E. Schauble, K.H. Desai, D. Bernstein, and B.K. Kobilka. 1999. Targeted disruption of the beta2 adrenergic

receptor gene. *J. Biol. Chem.* 274:16694–16700. doi:10.1074/jbc.274.24.16694

Crocker, P.R., and S. Gordon. 1986. Properties and distribution of a lectin-like hemagglutinin differentially expressed by murine stromal tissue macrophages. *J. Exp. Med.* 164:1862–1875. doi:10.1084/jem.164.6.1862

Dexter, T.M., M.A. Moore, and A.P. Sheridan. 1977. Maintenance of hemopoietic stem cells and production of differentiated progeny in allogeneic and semiallogeneic bone marrow chimeras in vitro. *J. Exp. Med.* 145:1612–1616. doi:10.1084/jem.145.6.1612

Frenette, P.S., S. Subbarao, I.B. Mazo, U.H. von Andrian, and D.D. Wagner. 1998. Endothelial selectins and vascular cell adhesion molecule-1 promote hematopoietic progenitor homing to bone marrow. *Proc. Natl. Acad. Sci. USA.* 95:14423–14428. doi:10.1073/pnas.95.24.14423

Giuliani, A.L., E. Wiener, M.J. Lee, I.N. Brown, G. Berti, and S.N. Wickramasinghe. 2001. Changes in murine bone marrow macrophages and erythroid burst-forming cells following the intravenous injection of liposome-encapsulated dichloromethylene diphosphonate (Cl2MDP). *Eur. J. Haematol.* 66:221–229. doi:10.1034/j.1600-0609.2001.066004221.x

Gordon, S., and P.R. Taylor. 2005. Monocyte and macrophage heterogeneity. *Nat. Rev. Immunol.* 5:953–964. doi:10.1038/nri1733

Hamilton, J.A. 2008. Colony-stimulating factors in inflammation and autoimmunity. *Nat. Rev. Immunol.* 8:533–544. doi:10.1038/nri2356

Hidalgo, A., A.J. Peired, L.A. Weiss, Y. Katayama, and P.S. Frenette. 2004. The integrin alphaMbeta2 anchors hematopoietic progenitors in the bone marrow during enforced mobilization. *Blood.* 104:993–1001. doi:10.1182/blood-2003-10-3702

Hume, D.A., A.P. Robinson, G.G. MacPherson, and S. Gordon. 1983. The mononuclear phagocyte system of the mouse defined by immunohistochemical localization of antigen F4/80. Relationship between macrophages, Langerhans cells, reticular cells, and dendritic cells in lymphoid and hematopoietic organs. *J. Exp. Med.* 158:1522–1536. doi:10.1084/jem.158.5.1522

Jung, S., J. Aliberti, P. Graemmel, M.J. Sunshine, G.W. Kreutzberg, A. Sher, and D.R. Littman. 2000. Analysis of fractalkine receptor CX(3)CR1 function by targeted deletion and green fluorescent protein reporter gene insertion. *Mol. Cell. Biol.* 20:4106–4114. doi:10.1128/MCB.20.11.4106-4114.2000

Jung, S., D. Unutmaz, P. Wong, G. Sano, K. De los Santos, T. Sparwasser, S. Wu, S. Vuthoori, K. Ko, F. Zavala, et al. 2002. In vivo depletion of CD11c+ dendritic cells abrogates priming of CD8+ T cells by exogenous cell-associated antigens. *Immunity.* 17:211–220. doi:10.1016/S1074-7613(02)00365-5

Katayama, Y., M. Battista, W.M. Kao, A. Hidalgo, A.J. Peired, S.A. Thomas, and P.S. Frenette. 2006. Signals from the sympathetic nervous system regulate hematopoietic stem cell egress from bone marrow. *Cell.* 124:407–421. doi:10.1016/j.cell.2005.10.041

Kiel, M.J., O.H. Yilmaz, T. Iwashita, C. Terhorst, and S.J. Morrison. 2005. SLAM family receptors distinguish hematopoietic stem and progenitor cells and reveal endothelial niches for stem cells. *Cell.* 121:1109–1121. doi:10.1016/j.cell.2005.05.026

Kiel, M.J., G.L. Radice, and S.J. Morrison. 2007. Lack of evidence that hematopoietic stem cells depend on N-cadherin-mediated adhesion to osteoblasts for their maintenance. *Cell Stem Cell.* 1:204–217. doi:10.1016/j.stem.2007.06.001

Liu, F., J. Poursine-Laurent, and D.C. Link. 2000. Expression of the G-CSF receptor on hematopoietic progenitor cells is not required for their mobilization by G-CSF. *Blood.* 95:3025–3031.

Lo Celso, C., H.E. Fleming, J.W. Wu, C.X. Zhao, S. Miake-Lye, J. Fujisaki, D. Cote, D.W. Rowe, C.P. Lin, and D.T. Scadden. 2009. Live-animal tracking of individual haematopoietic stem/progenitor cells in their niche. *Nature.* 457:92–96. doi:10.1038/nature07434

Lucas, D., M. Battista, P.A. Shi, L. Isola, and P.S. Frenette. 2008. Mobilized hematopoietic stem cell yield depends on species-specific circadian timing. *Cell Stem Cell.* 3:364–366. doi:10.1016/j.stem.2008.09.004

Marino, M.W., A. Dunn, D. Grail, M. Inglese, Y. Noguchi, E. Richards, A. Jungbluth, H. Wada, M. Moore, B. Williamson, et al. 1997. Characterization of tumor necrosis factor-deficient mice. *Proc. Natl. Acad. Sci. USA.* 94:8093–8098. doi:10.1073/pnas.94.15.8093

Méndez-Ferrer, S., and P.S. Frenette. 2007. Hematopoietic stem cell trafficking: regulated adhesion and attraction to bone marrow microenvironment. *Ann. N.Y. Acad. Sci.* 1116:392–413. doi:10.1196/annals.1402.086

Méndez-Ferrer, S., D. Lucas, M. Battista, and P.S. Frenette. 2008. Haematopoietic stem cell release is regulated by circadian oscillations. *Nature.* 452:442–447. doi:10.1038/nature06685

Méndez-Ferrer, S., M. Battista, and P.S. Frenette. 2010a. Cooperation of beta(2)- and beta(3)-adrenergic receptors in hematopoietic progenitor cell mobilization. *Ann. N.Y. Acad. Sci.* 1192:139–144. doi:10.1111/j.1749-6632.2010.05390.x

Méndez-Ferrer, S., T.V. Michurina, F. Ferraro, A.R. Mazloom, B.D. MacArthur, S.A. Lira, D.T. Scadden, A. Ma'ayan, G.N. Enikolopov, and P.S. Frenette. 2010b. Mesenchymal and haematopoietic stem cells form a unique bone marrow niche. *Nature.* 466:829–834. doi:10.1038/nature09262

Mignone, J.L., V. Kukekov, A.S. Chiang, D. Steindler, and G. Enikolopov. 2004. Neural stem and progenitor cells in nestin-GFP transgenic mice. *J. Comp. Neurol.* 469:311–324. doi:10.1002/cne.10964

Miyake, Y., K. Asano, H. Kaise, M. Uemura, M. Nakayama, and M. Tanaka. 2007. Critical role of macrophages in the marginal zone in the suppression of immune responses to apoptotic cell-associated antigens. *J. Clin. Invest.* 117:2268–2278. doi:10.1172/JCI31990

Oetke, C., G. Kraal, and P.R. Crocker. 2006. The antigen recognized by MOMA-I is sialoadhesin. *Immunol. Lett.* 106:96–98. doi:10.1016/j.imlet.2006.04.004

Omatsu, Y., T. Sugiyama, H. Kohara, G. Kondoh, N. Fujii, K. Kohno, and T. Nagasawa. 2010. The essential functions of adipo-osteogenic progenitors as the hematopoietic stem and progenitor cell niche. *Immunity.* 33:387–399. doi:10.1016/j.immuni.2010.08.017

Ralph, P., M.K. Ho, P.B. Litcofsky, and T.A. Springer. 1983. Expression and induction in vitro of macrophage differentiation antigens on murine cell lines. *J. Immunol.* 130:108–114.

Raschke, W.C., S. Baird, P. Ralph, and I. Nakoinz. 1978. Functional macrophage cell lines transformed by Abelson leukemia virus. *Cell.* 15:261–267. doi:10.1016/0092-8674(78)90101-0

Rosenthal, R.A., J.F. Megyesi, W.J. Henzel, N. Ferrara, and J. Folkman. 1990. Conditioned medium from mouse sarcoma 180 cells contains vascular endothelial growth factor. *Growth Factors.* 4:53–59. doi:10.3109/08977199009011010

Semerad, C.L., M.J. Christopher, F. Liu, B. Short, P.J. Simmons, I. Winkler, J.P. Levesque, J. Chappel, F.P. Ross, and D.C. Link. 2005. G-CSF potently inhibits osteoblast activity and CXCL12 mRNA expression in the bone marrow. *Blood.* 106:3020–3027. doi:10.1182/blood-2004-01-0272

Sugiyama, T., H. Kohara, M. Noda, and T. Nagasawa. 2006. Maintenance of the hematopoietic stem cell pool by CXCL12-CXCR4 chemokine signaling in bone marrow stromal cell niches. *Immunity.* 25:977–988. doi:10.1016/j.immuni.2006.10.016

Susulic, V.S., R.C. Frederich, J. Lawitts, E. Tozzo, B.B. Kahn, M.E. Harper, J. Himms-Hagen, J.S. Flier, and B.B. Lowell. 1995. Targeted disruption of the beta 3-adrenergic receptor gene. *J. Biol. Chem.* 270:29483–29492. doi:10.1074/jbc.270.49.29483

Van Rooijen, N., and A. Sanders. 1994. Liposome mediated depletion of macrophages: mechanism of action, preparation of liposomes and applications. *J. Immunol. Methods.* 174:83–93. doi:10.1016/0022-1759(94)90012-4

Wilson, A., and A. Trumpp. 2006. Bone-marrow haematopoietic-stem-cell niches. *Nat. Rev. Immunol.* 6:93–106. doi:10.1038/nri1779

Winkler, I.G., N.A. Sims, A.R. Pettit, V. Barbier, B. Nowlan, F. Helwani, I.J. Poulton, N. van Rooijen, K.A. Alexander, L.J. Raggatt, and J.P. Levesque. 2010. Bone marrow macrophages maintain hematopoietic stem cell (HSC) niches and their depletion mobilizes HSC. *Blood.* 116:4815–4828.

Zhang, J.Q., B. Biedermann, L. Nitschke, and P.R. Crocker. 2004. The murine inhibitory receptor mSiglec-E is expressed broadly on cells of the innate immune system whereas mSiglec-F is restricted to eosinophils. *Eur. J. Immunol.* 34:1175–1184. doi:10.1002/eji.200324723

Zhu, J., R. Garrett, Y. Jung, Y. Zhang, N. Kim, J. Wang, G.J. Joe, E. Hexner, Y. Choi, R.S. Taichman, and S.G. Emerson. 2007. Osteoblasts support B-lymphocyte commitment and differentiation from hematopoietic stem cells. *Blood.* 109:3706–3712. doi:10.1182/blood-2006-08-041384